SMALL NEGATIVE CLOUD-TO-GROUND LIGHTNING REPORTS AT THE KSC-ER

*Jennifer G. Wilson,[1,2] Kenneth L. Cummins[1,3] and E. Philip Krider[1]

[1]Institute of Atmospheric Physics, University of Arizona, Tucson, Arizona

[2]Also National Aeronautics and Space Administration/Kennedy Space Center, Florida

[3]Also Vaisala, Tucson, Arizona

Abstract

The NASA Kennedy Space Center (KSC) and Air Force Eastern Range (ER) use data from two cloud-to-ground (CG) lightning detection networks, the CGLSS and the NLDN, and a volumetric lightning mapping array, LDAR, to monitor and characterize lightning that is potentially hazardous to ground or launch operations. Data obtained from these systems during June-August 2006 have been examined to check the classification of small, negative CGLSS reports that have an estimated peak current, $|I_p|$ less than 7 kA, and to determine the smallest values of I_p that are produced by first strokes, by subsequent strokes that create a new ground contact (NGC), and by subsequent strokes that remain in a pre-existing channel (PEC). The results show that within 20 km of the KSC-ER, 21% of the low-amplitude negative CGLSS reports were produced by first strokes, with a minimum I_p of -2.9 kA; 31% were by NGCs, with a minimum I_p of -2.0 kA; and 14% were by PECs, with a minimum I_p of -2.2 kA. The remaining 34% were produced by cloud pulses or lightning events that we were not able to classify.

. *Corresponding author address*:
Jennifer G. Wilson, NASA KSC, KT-C-H, Kennedy Space Center, FL 32899;
E-mail: Jennifer.G.Wilson@nasa.gov.

1. Introduction

The NASA Kennedy Space Center (KSC) and Air Force Eastern Range (ER) are located in central Florida, a region that experiences a high area density of lightning flashes, and because of this, the KSC-ER use data from three lightning detection systems to monitor potential hazards to space launches and to provide warnings for ground operations. These systems consist of two cloud-to-ground (CG) lightning locating systems, the Cloud-to-Ground Lightning Surveillance System (CGLSS) and the U.S. National Lightning Detection Network™ (NLDN), and one 3-dimensional VHF lightning mapping array, the Lightning Detection and Ranging (LDAR) system, that detects air breakdown processes in intracloud and CG lightning. For operational applications at the KSC-ER, it is important to understand the performance of each detection system in considerable detail. It is also of scientific interest to know the smallest peak current, I_p, that can reach the ground, either in the form of the first return stroke in a CG flash or a subsequent stroke that creates a new ground contact (NGC), because low amplitude strokes might bypass a conventional lightning protection system that relies on a large attractive radius to prevent "shielding failure" (Golde, 1977; Uman, 2008). From the practical point of view, low amplitude strokes are difficult to detect, and because of this, they usually have larger location errors than larger events (Jerauld et al., 2005). Biagi et al (2007) studied 52 low amplitude ($|I_p| \leq 10$ kA), negative NLDN reports in southern Arizona, northern Texas, and southern Oklahoma, and found that only 50% to 87% were produced by CG strokes (either the first or a subsequent stroke in the flash) on the basis of video and waveform recordings. On the other hand, Fleenor et al (2009) studied 172 low amplitude ($|I_p| \leq 10$ kA), negative NLDN reports in the Central Great Plains, and found that only 15% were produced by CG strokes with the remaining 85% being cloud pulses. We have examined 260 CGLSS reports of small negative CG strokes at the KSC-ER during the summer of 2006 together with data from the other lightning detection systems to determine the type of lightning process that produced the report and the values of the estimated peak current, I_p. The CGLSS dataset is ideal for this purpose because the sensors have medium gain and relatively short baselines, so they are capable of detecting low-I_p strokes and locating them accurately over the KSC-ER (Wilson et al., 2009).

2. Instrumentation

2.1 Cloud-to-Ground Lightning Surveillance System (CGLSS)

The CGLSS contains 6 medium-gain IMPACT ESP sensors[1] placed at the locations shown in Figure 1. The CGLSS data are processed in the following sequence: 1) two or more remote sensors detect an electromagnetic waveform that is characteristic of a return stroke in CG lightning; 2) the GPS time, and the stroke amplitude, polarity, and magnetic direction are transmitted via land-line communications to a central processor; 3) the central processor uses time-coincident data from two or more sensors to compute an optimum stroke location and an estimate of the peak current, I_p, that is based on the range-normalized signal amplitude; and 4) the lightning information is forwarded to users in real-time via terrestrial data links. Included in these data are the value of a normalized chi-square (χ^2) error function at the optimum location and the size and orientation of a confidence ellipse that describes the accuracy of the location (Cummins et al., 1998). The value of χ^2 is a normalized measure of the "agreement" among all reporting sensors. Ideally, the distribution of χ^2 values has a mean and median of unity, but values between 0 and 3 are considered to be "good," and values between 3 and 10 are "acceptable." The semi-major and semi-minor axes of the confidence ellipse characterize the dimensions of a region that contains the actual stroke location (to within a given probability), and are based on a two-dimensional Gaussian distribution of location errors that are inferred from known measurement errors and the geometry of the sensor locations [see Cummins et al. (1998)]. The CGLSS uses a 37% (1/e) confidence region, and this corresponds to a 2-dimensional, one-standard-deviation location error (P = 0.37) of about 250 m (Wilson et al., 2009).

[1] Manufactured by Vaisala,Tucson, AZ

2.2 National Lightning Detection Network (NLDN)

The NLDN contains 113 high-gain IMPACT ESP sensors[1] placed 200-350 km apart so that they cover the continental U.S. (Cummins et al., 1998; 2006). Figure 2 shows the locations of the 10 nearest NLDN sensors to the KSC-ER (black triangles) and our analysis region (circled). Note that two of the three closest NLDN sensors are in Tampa and Ocala, FL, and that these are more than 200 km from the KSC-ER. The NLDN data are processed in a fashion that is generally similar to the CGLSS, except that satellite data links are used instead of land-line communications, and the central processor is in Tucson, AZ. The NLDN data for each stroke contain the GPS date and time (in ms); the optimum latitude and longitude; the magnitude of I_p and its polarity; the value of χ^2; the semi-major axis (SMA) in km and the orientation of the confidence ellipse; and the number of sensors that reported the stroke. The size of the NLDN confidence region is set to the median location error (i.e. P = 0.50) which is typically about 600 m at the KSC-ER (Wilson, et al., 2009). The average NLDN flash detection efficiency (DE) is typically better than 90% within the perimeter of the network, although the performance decreases somewhat near the boundaries (Cummins et al., 2006; Wilson et al., 2009).

At the time of this study, the CGLSS and NLDN systems differed somewhat in their reporting of the lightning information. The CGLSS reported the location of the first stroke in each flash and a portion of the subsequent strokes that struck ground more than about 500 m from the first-stroke (Maier and Wilson, 1996). Here, we will refer to both of these types of events as "CGLSS strokes." The NLDN on the other hand located all strokes that were reported by two or more sensors, and then (optionally) grouped them into flashes. Although both networks computed I_p using the peak radiation field (measured by sensors with the same bandwidth), the CGLSS computed I_p by multiplying the average value of all time-correlated, range-normalized signal strengths (in internal "LLP units") by a calibration factor of 0.23. The NLDN computed the I_p for each stroke by multiplying the average value of all time-correlated, range-normalized signal strengths reported by sensors that were within 625 km of the stroke location, and it used a calibration factor of 0.185 (Cummins et al., 2006). If the CGLSS detected more than one stroke in the flash at the same location, it reported the largest I_p of any stroke at that location, whereas the NLDN reported the I_p of the first stroke (unless all strokes were requested). In the following analyses, we have scaled all CGLSS values of I_p to make them consistent with the NLDN values because the NLDN has recently been "calibrated" on rocket-triggered subsequent strokes (Jerauld et al., 2005, Cummins et al., 2006). The required scaling, determined by Wilson et al. (2009) over the range of $\pm$150 kA, lowered the CGLSS values by a factor of 1.13. The time that was reported by the CGLSS is the time that the stroke waveform crossed a fixed detection threshold at the nearest reporting sensor, and the time that was reported by the NLDN is the time-of-occurrence of the stroke at the optimum stroke location. Therefore, the CGLSS times-of-occurrence can be up to 200 μs after the NLDN times in the evaluation region.

It is important to note that there is little experimental data that can be used to evaluate errors in the NLDN-based peak current estimates for negative strokes that create a new ground contacts (i.e. first strokes and subsequent strokes that create new ground terminations) and for all positive strokes, although Jerauld et al. (2007) suggest that the simple transmission line model accurately represents the current-to-field relationship in new ground contacts. Comparative analyses of direct measurements of the peak currents and peak fields suggest that NLDN-based estimates of I_p (calibrated on negative subsequent strokes in pre-existing channels) may under-estimate the true peak currents in first strokes and strokes that create new ground contacts, due to a slower return-stroke speed of propagation (Nag et al., 2008)

2.3 Lightning Detection And Ranging (LDAR) System

The LDAR system is a volumetric VHF lightning mapping array that contains 7 time-of-arrival (TOA) receivers at the locations shown in Figure 3. This system locates the sources of large radio impulses (centered at 66 MHz with a 6 MHz bandwidth) and has a median location accuracy of about 100m within 3 km of the LDAR central site (Maier et al., 1995). The primary sources of lightning VHF radiation are thought to be the stepped-leaders and other processes associated with the electrical breakdown of virgin air. The LDAR data consisted of the GPS date and time, together with the latitude, longitude, and altitude (in meters), of each VHF pulse that the LDAR system located during the flash. The LDAR flash detection efficiency is close to 100%, and the false alarm rate is less than 1% (Maier et al, 1995). For a more details about the LDAR system and its performance see Lennon and Maier (1991), Maier et al. (1995), and Boccippio et al. (2000a,b).

2.4 Los Alamos Sferic Array (LASA)

In addition to the LDAR dataset, we also examined a number of time-correlated electric field waveforms that were recorded by the Los Alamos Sferic Array (Smith et al., 2002, Shao et al., 2006). The LASA records broadband electromagnetic pulses from lightning in support of the radio frequency and optical observations of the Fast On-orbit Recording of Transient Events (FORTE) satellite. The Florida array contains 8 sensors connected to the internet, and the operation, data retrieval, and data processing are done at Los Alamos, NM (Shao et al., 2006). The closest LASA sensors to the KSC-ER are in Daytona Beach, Tampa, and Jacksonville, FL, but of these three sites, only Tampa was operating during our analysis period. Tampa is located about 200km west of the KSC-ER, and because of this large distance, most of the small CGLSS reports were below the detection threshold (~ 0.5 V/m) of the Tampa LASA sensor.

3. Methods

We examined a specific subset of 4967 negative lightning events that were reported by the CGLSS during the summer of 2006 (June 1 to August 31) and were located within 20 km of the LDAR central site shown in Figure 3. The NLDN and LDAR systems were used to check the classification of each report, i.e. whether it was produced by the first stroke in a CG flash, a subsequent stroke that created a new ground contact (NGC), a subsequent stroke that remained in a pre-existing channel (PEC), or a cloud pulse or some other lightning process that the CGLSS misclassified as a CG stroke. We also required that each CGLSS stroke be separated from any previous CGLSS report by at least 0.5 seconds in time and 2.0 km in space. Using these selection criteria, a total of 260 low-amplitude "candidate" first strokes and subsequent strokes that produced new ground-contacts remained out of the original 4967 events. Within the sample of 260 low amplitude CGLSS reports (i.e. with $|I_p| < 7$kA), 134 were detected by the LDAR system and/or the NLDN. These correlated events were then analyzed in greater detail.

A correction factor was applied to the CGLSS values of I_p using a "best-match" to the NLDN estimates as discussed in section 2.2. Figure 4 shows a plot of the (corrected) CGLSS I_p values (y-axis) vs. the NLDN I_p values (x-axis) for 82 low-amplitude, negative reports that were time-correlated to within 1 ms. The dotted line in figure 4 is the "slope=1" line, and it is clear that most of the observations are above this line. This offset is minimized (in the least-square-error sense) by adding 330 A to each NLDN value, and the result is shown by the solid line. The root-mean-square deviation of the CGLSS values about this line is 250 A. We note that the best-fit linear regression (slope and offset) to these data (not shown) results in the equation [$y = 0.887x - 0.298$] with a mean-square deviation of 240 A. These values provide an upper bound on the sum of the variances of the NLDN and CGLSS measurements. If we make the conservative assumption that the variance in the CGLSS values is half of the total variance, then the expected error in the GCLSS values of I_p has a standard deviation of $(0.25/2)^{1/2} = 353$ A, with a possible bias error (too small) of 330 A.

In order to analyze coincident events in the CGLSS and LDAR datasets, all LDAR sources that were in the region, and within a one-second time-interval that included the time of the CGLSS report, were plotted as a function of altitude and time as shown in Figure 5a. Here and in figures 6a to 9a to follow, the grey dots show the altitudes and times of the LDAR sources, and the symbols show the times that the CGLSS (squares) and the NLDN (triangles) reported strokes. In an LDAR record, a typical CG flash begins as a "line" of sources that moves from high to low altitudes (in tens of milliseconds) as the stepped-leader progresses toward ground, and two such leaders are evident in Figure 5a. We have noticed that leaders associated with strokes that produce a large $|I_p|$ tend to have more LDAR sources and a better-defined line moving toward the ground than strokes with a low $|I_p|$, and strokes that have a low $|I_p|$ may have only one or two LDAR sources preceding the CGLSS event at low altitudes. Most of the other VHF sources in an LDAR plot are produced by the development of negative branches and new channels inside the cloud (Mazur et al., 1997). In Fig. 5a, the CGLSS stroke-of-interest (SoI) is shown as a solid square at a height of 0 km. Any other CGLSS or NLDN reports that occurred within 20 km of the SoI in the interval of interest are plotted as open squares or solid triangles, respectively. If the NLDN reported the SoI, that event is plotted as a solid triangle directly above the CGLSS event at a height of 2000 m.

Figure 5b shows a plan view of the x-y positions of the same LDAR sources and the same CGLSS and NLDN locations that have been plotted in Figure 5a. Here and in Figures 6b to 9b to follow, the origin of the graph is at the LDAR central station (see Figure 3). Note in Figure 5b that the SoI struck ground about 9 km southwest of the first stroke, and that the third and fourth strokes (located by the NLDN) are much closer to the first stroke. Therefore, we believe that this was a multiple-stroke flash and that the second stroke created a NGC about 9 km SW of the first stroke. The third and fourth strokes remained within or near the original ground termination that was established by the first stroke.

Two aspects of Figures 5a and 5b indicate that the SoI was a subsequent stroke that produced a NGC: first, Figure 5a shows evidence of a stepped leader just prior to the SoI at 18:54:36.637 UTC, and second, there is a large separation (9 km) between the SoI and all the other strokes in Figure 5b. In cases like this, the probable location errors, derived from the SMA of the confidence ellipse and the χ^2 parameters, were used to determine if the difference in stroke positions could be due to random errors in the locating systems. If the confidence ellipse is large, then a large spatial separation between strokes is likely due to "expected" random errors. If the χ^2 is large (>5), then the expected location error is likely larger than the SMA, either because there were unusually-large measurement errors or because the report was caused by a cloud discharge.

Figure 5c shows the electric field waveform that was produced by the SoI and was recorded by the Tampa LASA sensor. Note that this waveform has many attributes of a return stroke that produced a new ground contact (i.e. a long initial rise-time and complex shape after the initial peak); therefore, our classification of the SoI as a subsequent stroke that produced a NGC is reasonable. This approach to classifying the CGLSS reports was refined and tested on several other of low-I_p events that had LASA waveforms to gain confidence that a proper classification could be assigned when the Tampa LASA sensor did not record the waveform.

4. Results

We will now show four more examples of low-Ip CGLSS events together with the LDAR and other data that have been used to classify them.

4.1 First Stroke in a Flash

Figure 6 shows an example of a -3.9 kA first stroke that occurred at 19:46:53.918 UTC on July 17, 2006. The time/height plot in Figure 6a shows that one or more attempted leaders developed prior to the leader that contacted ground at 53.918 seconds. The minimum χ^2 values at the CGLSS and NLDN locations were both good (0.7 and 2.0, respectively) and the median SMAs of the CGLSS and NLDN confidence ellipses were 0.18 nm (0.33 km) and 1.7 km, respectively. A larger SMA at the NLDN location was expected because the NLDN sensors are spaced about 10 times further apart than the CGLSS sensors, and low-current strokes at the KSC-ER are typically seen by only 2 or 3 NLDN sensors. The difference in locations in Figure 6b is about 3.5 km, but this difference is reasonable given the large NLDN SMA. The nearest prior CGLSS report occurred 3.736 seconds before the event shown in Figure 6 and was 226 km from the origin.

28 reports (21%) of the 134 low-amplitude CGLSS strokes in our dataset were determined to be for first strokes in CG flashes (like Figure 6). Characteristics of the storm cells (developing, mature, or decaying) that were associated with all 28 of these strokes were tabulated and compared to determine if there was any tendency for small or developing storms to produce small strokes, and none was found, i.e.15 events

occurred in small, developing, or decaying cells, and 13 events were associated with large, mature storms.

4.2 Subsequent Strokes that Produced a New Ground Contact (NGC)

41 (31%) of the low-amplitude CGLSS reports were determined to be for subsequent strokes that produced a new ground contact (NGC), and we have previously shown an example of this type of event in Figure 5. Figure 7 shows another example of a subsequent stroke that produced a NCG on August 23, 2006. The LDAR time/height plot in Figure 7a shows evidence of leaders propagating toward ground before the first stroke and before the SoI. The CGLSS and NLDN both reported the SoI and the I_p values were -6.0 kA and -6.4 kA, respectively. The chi-square values at the optimum CGLSS and NLDN locations were both good (0.3 and 1.4, respectively) and the SMAs at the CGLSS and NLDN locations were 0.1nm (0.19 km) and 2.8 km, respectively. The classification of the SoI as a NGC is supported by the facts that it was 3.4 km from an accurately located (χ^2 = 0.3; SMA = 0.19 km) first stroke in Figure 7b, the expected location errors were small, and there were a few low-altitude LDAR sources just prior to the second stroke. Based on the NLDN, the location of the third stroke was likely the same as the second stroke.

4.3 Subsequent Strokes that Remained in a Pre-Existing Channel (PEC)

19 (14%) of the CGLSS strokes in our dataset were classified as subsequent strokes that remained within or very close to a pre-existing channel (PEC). Figure 8 shows an example of the LDAR sources and locations of a -3.3 kA subsequent stroke that was classified as a PEC on July 18, 2006. The time/height plot in Figure 8a shows a clear leader propagating to ground before the first stroke, and there is no evidence of a leader before the SoI. The NLDN detected the first stroke, and it did not detect the SoI. The value of χ^2 was good (0.2), the SMA was only 0.20 nm (0.37 km); and the event was reported by only 2 CGLSS sensors. The classification as a subsequent stroke that remained in a PEC is supported by the

relatively short time-interval between the first stroke and the SoI, the lack of LDAR leader pulses before the SoI, the large SMA, and the small number of CGLSS sensors that reported the event. The first stroke in this flash occurred 36 ms before the SoI and had an I_p of -13.7 kA.

4.4 Cloud Pulses and CGLSS Reports That Could Not Be Classified

32 (24%) of the low-amplitude CGLSS strokes in our dataset were determined to be for cloud pulses, and 14 (10%) of the reports were produced by lightning processes that we were not able to classify. Figure 9 shows an example of a -4.2 kA (equivalent I_p) cloud pulse that occurred on July 7, 2006. In an LDAR record, a cloud discharge often begins with an initial upward movement of sources, and the time/height plot in Figure 9a shows LDAR sources moving upward from about 8 km to 14 km just at the time of the CGLSS report. In this case, the CGLSS was not able to compute a chi-square value because the arrival-times were not consistent and the location was derived from the intersection of just two direction vectors. The SMA was 0.37 nm (0.69 km), and the nearest prior CGLSS report was 6.641 sec before the SoI and 40.4 km from the origin. The NLDN did not report this event.

4.5 Minimum Values of the Inferred Peak Current, I_p

Of the 88 small CGLSS events that were classified as CG strokes in the analysis region, the lowest I_p for a first stroke was -2.9 kA; the lowest I_p for a subsequent stroke that produced a NGC was -2.0 kA; and the lowest Ip for a subsequent stroke that remained in a PEC was -2.2 kA. Figure 10 shows histograms of the CGLSS $|I_p|$ values for each type of ground stroke. Here, it is important to note that 23 (26%) of the 88 CG strokes in our dataset had an $|I_p|$ less than 4.0 kA, and of these, 11 were NGCs and only 6 were first strokes. 20 CG strokes had an $|I_p|$ between 4.0 and 5.0 kA, and of these, only one was a first stroke.

Figure 11 shows a distribution similar to Figure 10, but for the 32 cloud pulses that the CGLSS misclassified as a CG stroke plus the 14 events that we were not able to classify.

From these results, we conclude that the Cloud-to-Ground Lightning Surveillance System at the KSC-ER has reported first strokes with an estimated peak current as low as -3 kA and subsequent strokes that produce new ground contacts with an I_p of about -2 kA, and that the frequency-of-occurrence of such events is low.

Summary

We have analyzed 134 low-amplitude, negative CGLSS reports (i.e. events with an $|I_p| < 7$ kA) that were within 20 km of the LDAR central site at the KSC-ER, and compared them with LDAR and NLDN data to determine the type of lightning process that produced these reports. 28 (21%) of the reports were produced by the first stroke in CG flashes, and there was no preference for the production of low-amplitude events during the early, mature, or final stages of storm development. Overall, 88 (66%) of the low-amplitude, negative reports were produced by cloud-to-ground strokes, and 60 (45%) of these were produced by subsequent strokes that either created a new ground contact or remained in a pre-existing channel. These findings are in good agreement with the results of Biagi et al. (2007) in AZ-TX-OK, except that Biagi et al. used a criterion of an $|I_p| \leq 10$ kA and found that 50-87% of the small NLDN reports could be classified as CG (either first or subsequent strokes) on the basis of video and waveform recordings. More recently, Fleenor et al (2009), using the same criterion as Biagi et al., have found that only 15% of the NLDN reports in the Central Great Plains were CG strokes and 85% were cloud pulses. The remaining 46 (34%) of the CGLSS reports at the KSC-ER were caused by cloud pulses (32) or lightning processes that we were not able to classify (14).

This work has also shown that the current CGLSS data processing algorithm does not identify new ground contacts properly because roughly 1 out of 7 CGLSS reports were actually CG strokes that occurred in PECs. This occurs when two or three of the CGLSS sensors have magnetic direction errors that are larger than one degree but agree with each other. This results in a single stroke being reported at two locations (by different sensors) that have a large position difference. A new CGLSS data processing algorithm that will correct this problem is now certified for operational use at the KSC-ER.

The smallest CGLSS $|I_p|$ for the first stroke in a flash was 2.9 kA, and the smallest $|I_p|$ for a subsequent stroke was 2.0 kA. Only 6 CGLSS first strokes had an $|I_p| < 4$ kA, and this number increased to 17 for $|I_p| < 5$ kA. Although these measurements are close to the CGLSS detection threshold, they do agree with direct measurements of negative lightning strikes to instrumented towers (Berger et al., 1975, reviewed by Rakov,1985) that show first strokes produce a minimum peak current of about -5kA and subsequent strokes in the same channel produce a minimum peak current near -2 kA. Our measurements also suggest that the minimum peak current of a negative subsequent stroke that creates a new ground contact is about -2 kA. Our discussions of minimum peak current must be considered in the light of the limitations expressed at the end of Section 2.3, as well as our expected measurement errors (353 A RMS random error with a possible bias error (too small) of 330 A)

Acknowledgements

One of the authors (JGW) has submitted this research in partial fulfillment of the requirements for an M.S. degree in atmospheric sciences at the University of Arizona. This work has been supported in part by the NASA Kennedy Space Center, Grant NNK06EB55G and by Vaisala, Tucson, AZ. The authors thank the Los Alamo National Laboratory for acquiring the LASA data.

NOTICE

Mention of a copyrighted, trademarked or proprietary product, service, or document does not constitute endorsement thereof by the author, the National Aeronautics and Space Administration, or the United

States Government. Any such mention is solely for the purpose of fully informing the reader of the resources used to conduct the work reported herein.

References

Berger, K., R. B. Anderson, and H. Kroninger, 1975: Parameters of lightning flashes. *Electra*, *80*, 223-237.

Biagi, C.J., K.L. Cummins, K.E. Kehoe, and E.P. Krider, 2007: National Lightning Detection Network (NLDN) performance in southern Arizona, Texas, and Oklahoma in 2003-2004. *J. Geophys. Res., 112*, D05208, doi:10.1029/2006JD007341.

Boccippio, D.J., S. Heckman, and S. J. Goodman, 2000a: A diagnostic analysis of the Kennedy Space Center LDAR network 1. Data characteristics. *J. Geophys. Res., 106*, 4769–4786.

Boccippio D.J., S. Heckman, and S. J. Goodman, 2000b: A diagnostic analysis of the Kennedy Space Center LDAR network 2. Cross-sensor studies. *J. Geophys. Res., 106,* 4787–4796.

Boyd, B.F., W.P. Roeder, D.L. Hajek, and M.B. Wilson, 2005: Installation, Upgrade, and Evaluation of a Short Baseline Cloud-to-Ground Lightning Surveillance System used to Support Space Launch Operations, AMS Conference on Meteorological Applications of Lightning Data, San Diego, CA, 9 – 13 January.

Cummins, K. L., J. A. Cramer, C. J. Biagi, E. P. Krider, J. Jerauld, M. A. Uman, and V.A. Rakov, 2006: The U.S. National Lightning Detection Network: Post-upgrade status, 2nd AMS Conference on Meteorological Applications of Lightning Data, Atlanta, GA, 29 January – 2 February.

Cummins, K.L., M.J. Murphy, E.A. Bardo, W.L. Hiscox, R.B. Pyle, and A.E. Pifer, 1998: A combined TOA/MDF technology upgrade of the U.S. National Lightning Detection. Network, *J. Geophys. Res.*, *98*, 9035-9044.

Fleenor, S.A., C.J. Biagi, K.L. Cummins, E.P. Krider, and X.M. Shao, 2009: Characteristics od cloud-to-ground lightning in warm-season thunderstorms in the Central Great Plains. *Atmos. Res.*, doi:10.1016/j.atmosres.2008.08.011.

Golde, R. H, 1977: *Lightning: Physics of Lightning*, Vol. 1,Academic Press, New York.

Jerauld, j., M.A. Uman, V.A. Rakov, K.J. Rambo, G.H. Schnetzer, 2007: Insights into the ground attachment process of natural lightning gained from an unusual triggered-lightning stroke, *J. Geophys. Res., 112*, D13113, doi:10.1029/2006/JD007682.

Jerauld J., V. A. Rakov, M. A. Uman, K. J. Rambo, D. M. Jordan, K. L. Cummins, J. A. Cramer, 2005: An evaluation of the performance characteristics of the U.S. National Lightning Detection Network in Florida using rocket-triggered lightning, *J. Geophys. Res., 110*, D19106, doi:10.1029/2005JD005924.

Lennon, C. and L. Maier, 1991: Lightning Mapping System, Proc. International Aerospace and Ground Conference on Lightning and Static Electricity (ICOLSE), Vol. II, Cocoa Beach, FL, 16-19 April.

Maier, L., C. Lennon, T. Britt, and S. Schaefer, 1995: Lightning Detection and Ranging (LDAR) System Performance Analysis. 6th Conference on Aviation Weather Systems, Dallas, TX.

Mazur, V., E. Williams, R. Boldi, L. Maier, D.E. Proctor, 1997: Initial comparison of lightning mapping with operational Time-of-Arrival and interferometric systems, *J. Geophys. Res.*, *102*, D10, pp. 11,071-11,085.

Nag, A., V. A. Rakov, W. Schulz, M. M. F. Saba, R. Thottappillil, C. J. Biagi, A. O. Filho, A. Kafri, N. Theethayi, and T. Gotsch, 2008: First versus subsequent return-stroke current and field peaks in negative cloud-to-ground lightning discharges, *J. Geophys. Res.*, *113*, doi:10.1029/2007JD009729,.

Rakov, V. A., 1985: On estimating the lightning peak current distribution parameters taking into account the lower measurement limit. *Elektrichestvo*, 2, 57-59.

Shao, X. M., M. Stanley, A. Regan, J. Harlin, M. Pongratz, and M. Stock, 2006: Total Lightning Observations with the New and Improved Los Alamos Sferic Array (LASA). *J. Atmos. Oceanic Technol.*, *23*, 1273-1288.

Smith, D. A., K. B. Eack, J. Harlin, M. J. Heavner, A. R. Jacobson, R. S. Massey, X. M. Shao, and K. C. Wiens, 2002: The Los Alamos Sferic Array: A research tool for lightning investigations. *J. Geophys. Res., 107*, D13, 4183, doi:10.1029/2001JD000502.

Uman, M.A. (2008), *The Art and Science of Lightning Protection*, Cambridge University Press, Cambridge, 240 p.

Wilson, J. G., K. L. Cummins, E. P. Krider, 2009: Comparison of the cloud-to-ground lightning surveillance system (CGLSS) and the U.S. National Lightning Detection Network™ (NLDN) at the KSC-ER, to be submitted to *J. Spacecraft and Rockets*.

Captions

Figure 1. Locations of the CGLSS sensors (triangles) at the KSC-ER in 2006 and our analysis region.

Figure 2. The locations of the NLDN sensors near the KSC-ER.

Figure 3. Locations of the LDAR sensors (black circles), the central station (open circle), and the analysis region (circled).

Figure 4. CGLSS I_p values vs. NLDN I_p values for 82 time-correlated, low-amplitude ($|I_p|$ <7kA) events that were detected by both networks within 20 km of the origin shown in Figure 3.

Figure 5a. Heights of LDAR sources as a function of time for a CGLSS event that was classified as a subsequent stroke that that produced a new ground contact (NGC) at 18:54:36.637 UTC on July 7, 2006. The stroke-of-interest (SoI) (shown by the open solid square) had an I_p of -3.1 kA, a χ^2 of 5.1, and the semi-major axis (SMA) of the confidence ellipse was 0.2nm (0.37 km). Four CGLSS sensors reported the event.

Figure 5b. Plan view of the LDAR sources and stroke locations shown in Figure 5a. The origin for the plot is the LDAR central station shown in Figure 3.

Figure 5c. The LASA waveform for the -3.1 kA CGLSS SoI shown in Figures 5a and 5b. Time starts at 18:54:36.637 UTC, and the electric field scale has not been calibrated.

Figure 6a. Heights of the LDAR sources as a function of time for a CGLSS event that occurred at 19:46:53.918 UTC on July 17, 2006 and was classified as a first stroke. The I_p was -3.9 kA, the χ^2 was 0.7, and the SMA of the confidence ellipse was 0.1nm (0.19 km). 5 CGLSS sensors reported the SoI.

Figure 6b. Plan view of the LDAR sources and the CGLSS and NLDN locations of the event shown in Figure 6a. (See also caption for Figure 5b.)

Figure 7a. Heights of the LDAR sources as a function of time for a CGLSS report that was classified as a subsequent stroke that produced a NGC at 21:18:39.418 UTC on August 23, 2006. In this case, the SoI had an I_p of -6.0 kA, the χ^2 was 0.3, the SMA was 0.1nm (0.19 km), and 5 sensors reported the event.

Figure 7b. Plan view of the LDAR sources and stroke locations for the event shown in Figure 7a. (See also caption for Figure 5b.)

Figure 8a. Heights of LDAR sources as a function of time for a subsequent stroke that remained in a pre-existing channel (PEC) at 17:18:39.257 UTC on July 18, 2006. The CGLSS I_p was -3.3 kA, the χ^2 was 0.2, the SMA was 0.2 nm (0.37 km), and 2 sensors reported the event.

Figure 8b. Plan view of the LDAR sources and stroke locations for the event shown in Figure 8a. (See also caption for Figure 5b.)

Figure 9a. Heights of the LDAR sources as a function of time for a cloud pulse that occurred at 18:46:39.533 UTC on July 7, 2006. The equivalent CGLSS I_p was -4.2 kA, the χ^2 was 0.0, the SMA was 0.37nm (0.69 km), and just 2 sensors reported the event.

Figure 9b. Plan view of the LDAR sources shown in Figure 9a. (See also caption for Figure 5b.)

Figure 10. Distributions of the CGLSS $|I_p|$ values for 28 low-amplitude first strokes, 41 strokes that produced a NGC, and 19 strokes that remained in a PEC.

Figure 11. Distribution of the CGLSS values of $|I_p|$ for 32 cloud pulses (solid) and 14 events (shaded) that could not be classified.

Figures

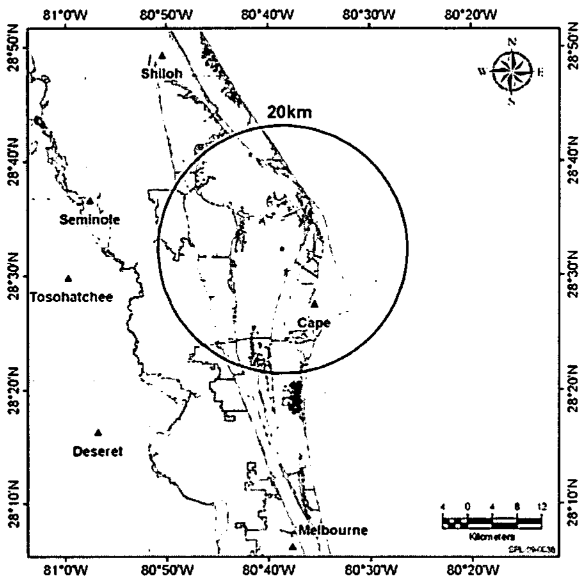

Figure 1. Locations of the CGLSS sensors (triangles) at the KSC-ER in 2006 and our analysis region.

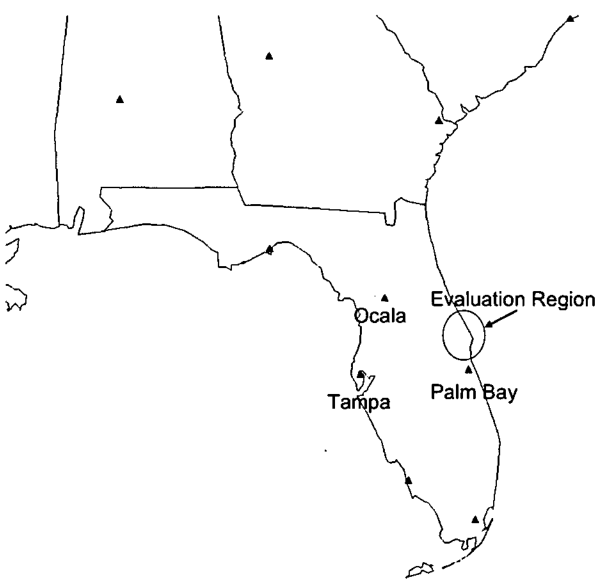

Figure 2. The locations of the NLDN sensors near the KSC-ER.

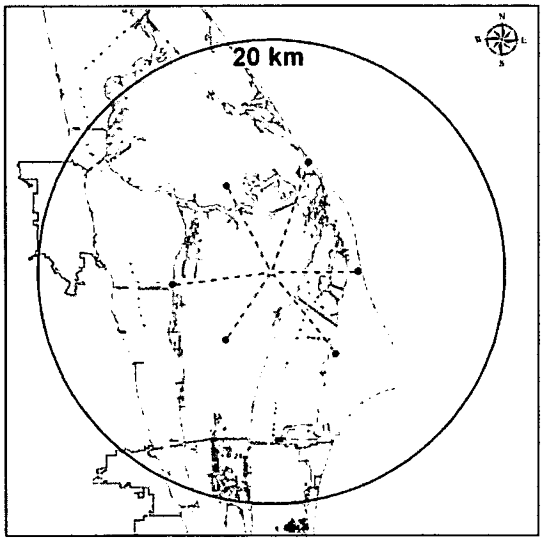

Figure 3. Locations of the LDAR sensors (black circles), the central station (open circle), and the analysis region (circled).

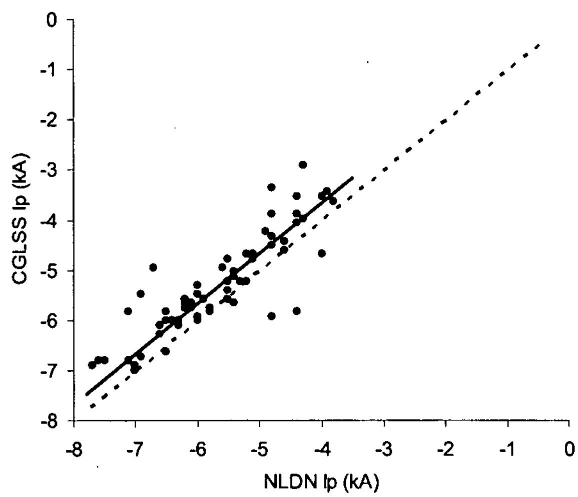

Figure 4. CGLSS I_p values vs. NLDN I_p values for 82 time-correlated, low-amplitude ($|I_p|$ <7kA) events that were detected by both networks within 20 km of the origin shown in Figure 3.

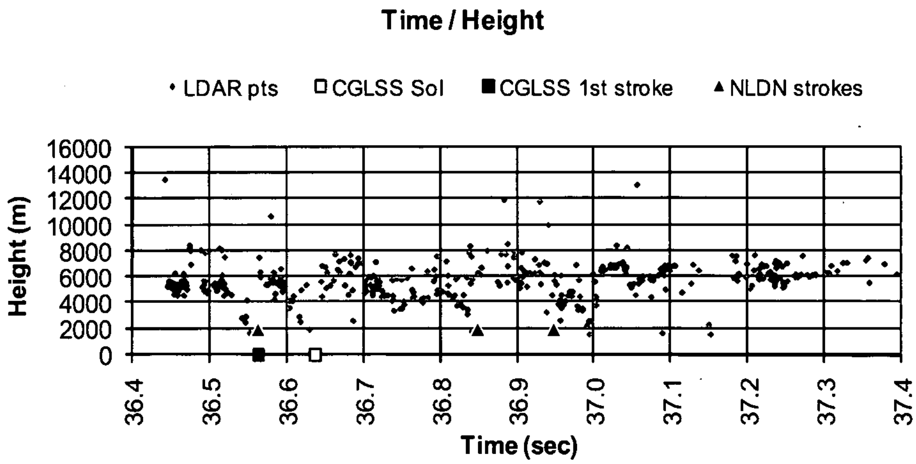

Figure 5a. Heights of LDAR sources as a function of time for a CGLSS event that was classified as a subsequent stroke that that produced a new ground contact (NGC) at 18:54:36.637 UTC on July 7, 2006. The stroke-of-interest (SoI) (shown by the open solid square) had an I_p of -3.1 kA, a χ^2 of 5.1, and the semi-major axis (SMA) of the confidence ellipse was 0.2nm (0.37 km). Four CGLSS sensors reported the event.

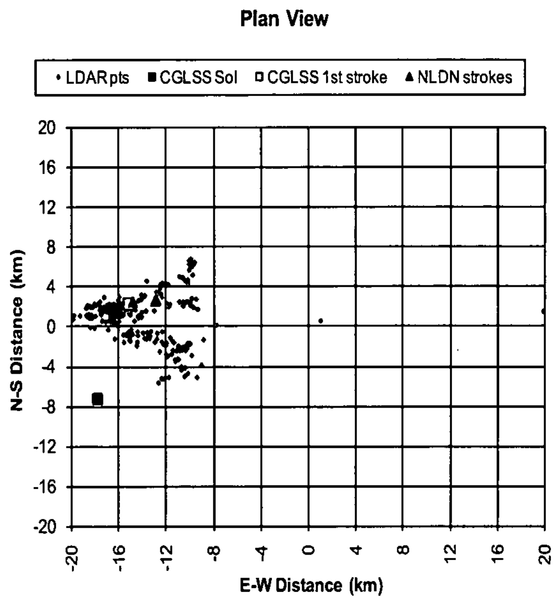

Figure 5b. Plan view of the LDAR sources and stroke locations shown in Figure 5a. The origin for the plot is the LDAR central station shown in Figure 3.

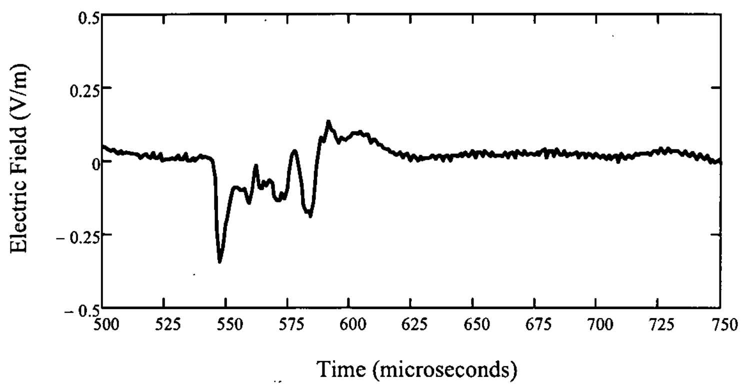

Figure 5c. The LASA waveform for the -3.1 kA CGLSS SoI shown in Figures 5a and 5b. Time starts at 18:54:36.637 UTC, and the electric field scale has not been calibrated.

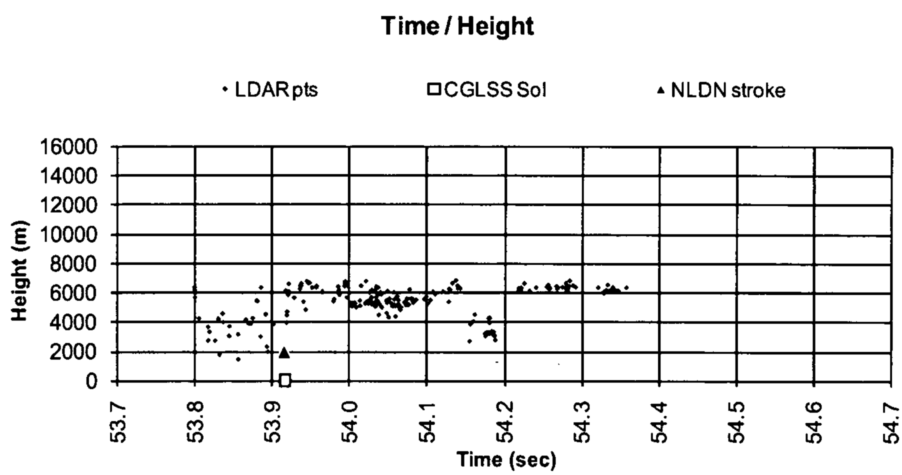

Figure 6a. Heights of the LDAR sources as a function of time for a CGLSS event that occurred at 19:46:53.918 UTC on July 17, 2006 and was classified as a first stroke. The I_p was -3.9 kA, the χ^2 was 0.7, and the SMA of the confidence ellipse was 0.1nm (0.19 km). 5 CGLSS sensors reported the SoI.

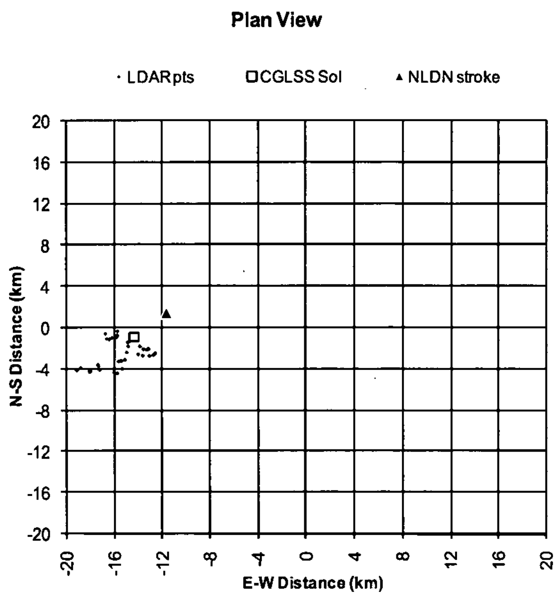

Figure 6b. Plan view of the LDAR sources and the CGLSS and NLDN locations of the event shown in Figure 6a. (See also caption for Figure 5b.)

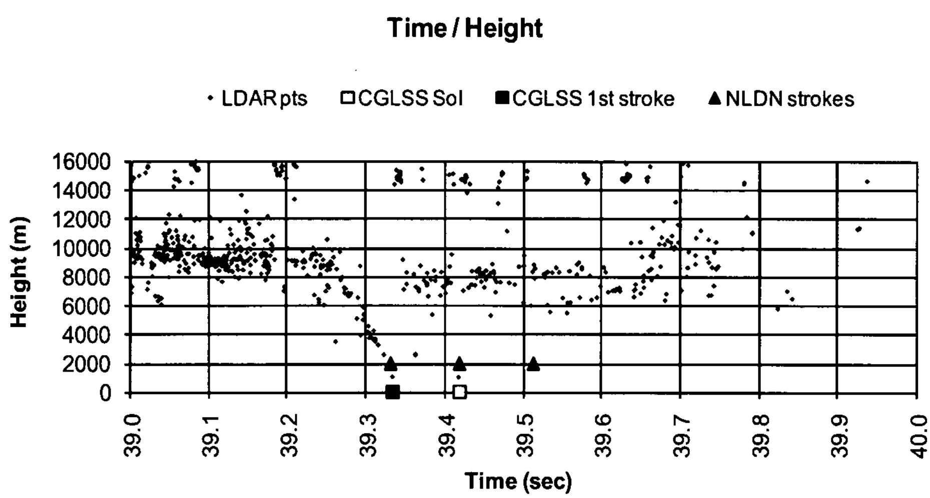

Figure 7a. Heights of the LDAR sources as a function of time for a CGLSS report that was classified as a subsequent stroke that produced a NGC at 21:18:39.418 UTC on August 23, 2006. In this case, the SoI had an I_p of -6.0 kA, the χ^2 was 0.3, the SMA was 0.1nm (0.19 km), and 5 sensors reported the event.

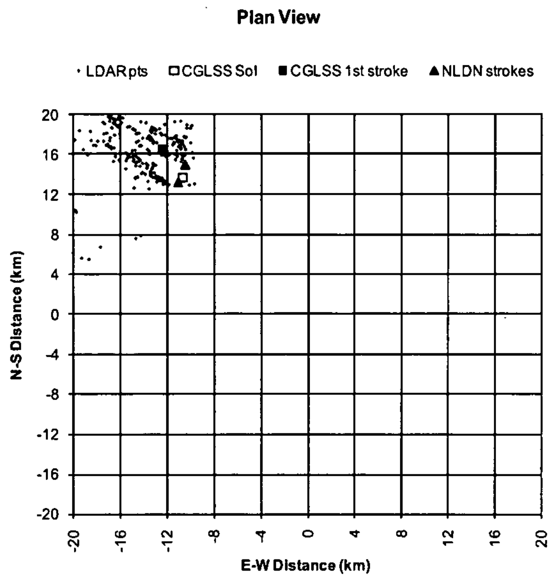

Figure 7b. Plan view of the LDAR sources and stroke locations for the event shown in Figure 7a. (See also caption for Figure 5b.)

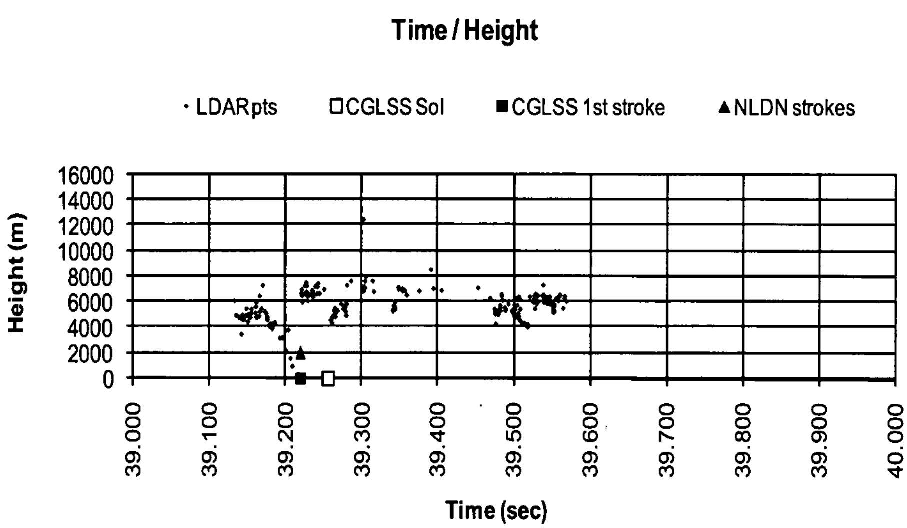

Figure 8a. Heights of LDAR sources as a function of time for a subsequent stroke that remained in a pre-existing channel (PEC) at 17:18:39.257 UTC on July 18, 2006. The CGLSS I_p was -3.3 kA, the χ^2 was 0.2, the SMA was 0.2 nm (0.37 km), and 2 sensors reported the event.

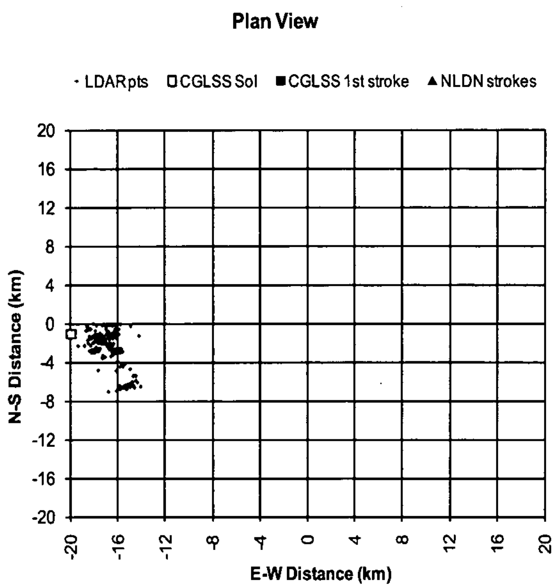

Figure 8b. Plan view of the LDAR sources and stroke locations for the event shown in Figure 8a. (See also caption for Figure 5b.)

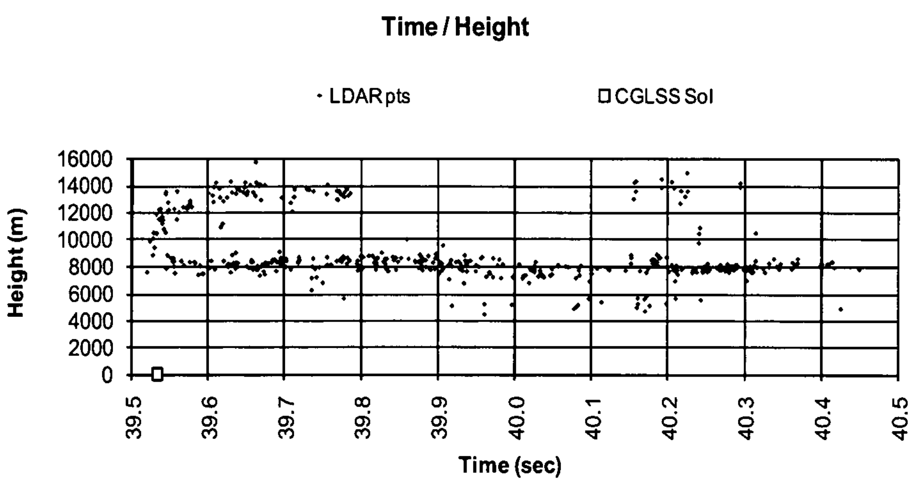

Figure 9a. Heights of the LDAR sources as a function of time for a cloud pulse that occurred at 18:46:39.533 UTC on July 7, 2006. The equivalent CGLSS I_p was -4.2 kA, the χ^2 was 0.0, the SMA was 0.37nm (0.69 km), and just 2 sensors reported the event.

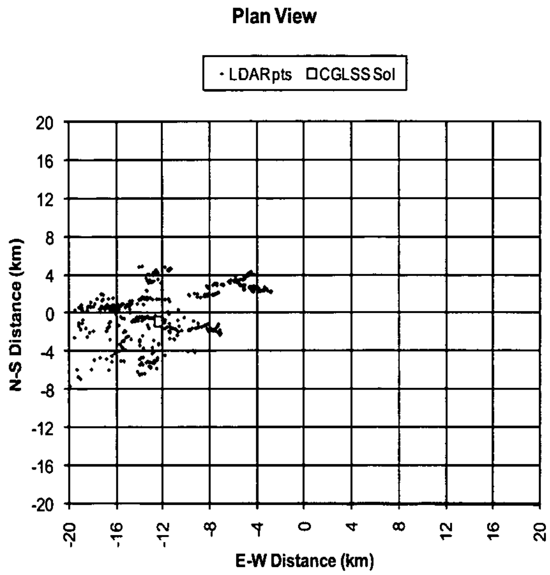

Figure 9b. Plan view of the LDAR sources shown in Figure 9a. (See also caption for Figure 5b.)

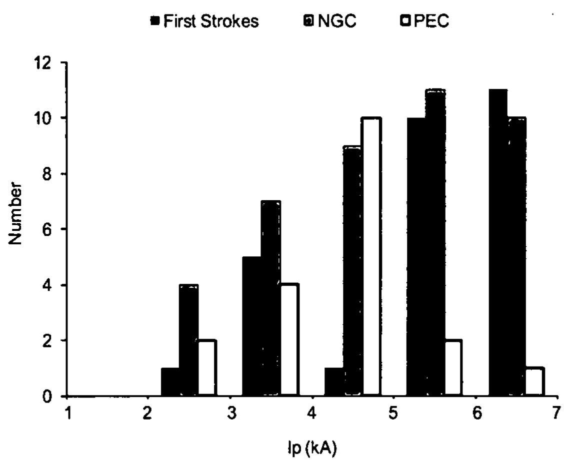

Figure 10. Distributions of the CGLSS $|I_p|$ values for 28 low-amplitude first strokes, 41 strokes that produced a NGC, and 19 strokes that remained in a PEC.

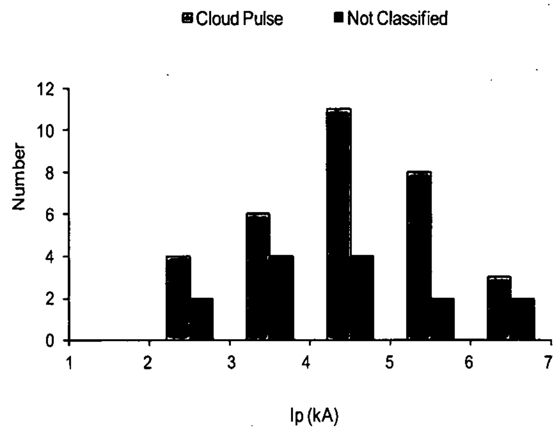

Figure 11. Distribution of the CGLSS values of $|I_p|$ for 32 cloud pulses (solid) and 14 events (shaded) that could not be classified.